



# Machine learning-based temporal change detection of land use and land cover changes in the Tunçbilek open pit coal mine region using PlanetScope imagery

## Planetscope görüntüleri kullanılarak Tunçbilek açık ocak kömür madeni bölgesinde arazi kullanım ve örtü değişikliklerinin makine öğrenmesi tabanlı zamansal değişim tespiti

Recep Uğur Acar<sup>1,\*</sup>, Enes Zengin<sup>2</sup>, Ali Samet Öngen<sup>3</sup>

<sup>1,3</sup> Kütahya Dumlupınar University, Geological Engineering Department, 43140, Kütahya, Türkiye

<sup>2</sup> Istanbul Technical University, Geological Engineering Department, 34469, Istanbul, Türkiye

### Abstract

This study investigates land use and land cover (LULC) changes in the Tunçbilek open-pit coal mine and its surroundings, a region experiencing intense mining activity in western Türkiye. Understanding LULC dynamics is crucial for assessing the long-term environmental impacts of surface mining operations and supporting sustainable land management. High-resolution PlanetScope imagery from 2016 and 2021 was used in conjunction with two supervised machine learning algorithms Maximum Likelihood Classification (MLC) and Support Vector Machine (SVM) to detect temporal changes in six land cover classes. The results show that SVM outperformed MLC in classification accuracy. The kappa values for MLC were 0.73 (2016) and 0.72 (2021), whereas SVM achieved 0.87 and 0.84, respectively. SVM also provided higher user and producer accuracy rates, particularly for the forest and planted classes. Between 2016 and 2021, notable land cover transitions were observed, including a 6.83% increase in cultivated lands and a 7.9% decrease in barren land. The mining area itself expanded by approximately 1.39%. These results highlight the effectiveness of machine learning-based remote sensing methods in monitoring LULC changes and contribute to a better understanding of the environmental impacts of mining activities in complex and sensitive landscapes.

**Keywords:** Change detection, Machine learning, Mining site, MLC, Planet Scope, Remote sensing, SVM

### 1. Introduction

Today's rapid economic and technological development has led to an increase in the demand for both mineral resources and energy, which in turn has led to the rise in the market for underground resources [1-5]. Coal from underground resources is one of the most critical energy resources due to its low cost and abundance compared to other resources both in the world and in our country,

### Öz

Bu çalışma, Batı Anadolu'da yoğun madencilik faaliyetlerinin yürütüldüğü bir bölge olan Kütahya'daki Tunçbilek açık ocak kömür madeni ve çevresindeki arazi kullanım ve örtü (LULC) değişimlerini incelemektedir. Yüze madenciliği operasyonlarının uzun vadeli çevresel etkilerinin değerlendirilmesi ve sürdürülebilir arazi yönetiminin desteklenmesi açısından LULC dinamiklerinin anlaşılması büyük önem taşımaktadır. Bu amaçla, 2016 ve 2021 yıllarına ait yüksek çözünürlüklü PlanetScope uydu görüntüleri kullanılmış ve zamansal değişimlerin tespiti için Maksimum Olabilirlik Sınıflandırması (MLC) ile Destek Vektör Makineleri (SVM) olmak üzere iki denetimli makine öğrenme algoritması uygulanmıştır. Elde edilen sonuçlara göre, sınıflandırma doğruluğu açısından SVM, MLC'ye kıyasla daha yüksek performans göstermiştir. MLC için kappa katsayıları 2016 yılında 0.73, 2021 yılında ise 0,72 olarak belirlenirken; SVM için bu değerler sırasıyla 0.87 ve 0.84 olarak hesaplanmıştır. Özellikle orman ve ekili alan sınıflarında SVM, kullanıcı ve üretici doğruluklarında daha yüksek başarı elde etmiştir. 2016-2021 yılları arasında tarım alanlarında %6.83'lük bir artış, çıplak toprak alanlarında ise %7.9'lük bir azalma gözlemlenmiştir. Madencilik alanı ise yaklaşık %1.39 oranında genişlemiştir. Bu bulgular, LULC değişimlerinin izlenmesinde makine öğrenmesi tabanlı uzaktan algılama yöntemlerinin etkinliğini ortaya koymakta ve karmaşık, hassas peyzajlarda madencilik faaliyetlerinin çevresel etkilerinin daha iyi anlaşılmasına katkı sağlamaktadır.

**Anahtar kelimeler:** Değişim tespiti, Makine öğrenmesi, Maden sahası, MLC, Planet Scope, SVM, Uzaktan algılama

especially in terms of electricity energy demand [1, 6-8]. Two main mining methods are employed for the extraction of coal and other mineral resources: underground and surface mining methods [9-12]. Coal mining is commonly carried out using open pit mining, which is carried out on the earth's surface [13-14]. The extraction of coal through open-pit mining inevitably entails the removal of overlying rock and soil material. This process results in alteration of the

\* Sorumlu yazar / Corresponding author, e-posta / e-mail: ugur.acar@dpu.edu.tr (R. U. Acar)

Geliş / Received: 13.01.2025 Kabul / Accepted: 22.05.2025 Yayınlanma / Published: 15.07.2025

doi: 10.28948/ngumuh.1619090

surrounding vegetation, water bodies and geography, and some instances, it also affects settlements [15-21]. Given the above impacts of opencast mining activities, Mining sites must be continuously monitored. This is vital for the sustainability of mining operations as it allows a precise understanding of the long-term environmental and land cover impacts and how changes to the surface are shaped over time [22]. This monitoring process enables the extent of soil erosion, vegetation loss, water resources status, and land use change to be revealed. It can be helpful for early detection of disaster risks such as landslides and subsidence [23]. Therefore, continuous and regular monitoring of these changes is necessary to support sustainable mining practices and minimize potential risks [24].

Traditional mining site monitoring techniques, such as topographic and photogrammetric surveys, are often time- and labour-intensive. Topographic measurements involve collecting elevation and landform data from various points on the site, requiring site visits and detailed measurements. Similarly, photogrammetric studies aim to create three-dimensional terrain models using aerial or drone images. However, data collection and analysis processes for these techniques could be more laborious and time-consuming in mining areas with large surface areas. In this context, remote sensing methods utilizing satellite data offer a highly cost-effective and beneficial approach for monitoring land use and land cover (LULC) changes across large geographical areas [22, 24-25]. Land cover refers to the uppermost layer of the Earth's surface, such as water, vegetation, bare soil, urban infrastructure, or any other surface feature [26-28]. In contrast, land use classification aims to define the functional purpose of the land, such as recreation, wildlife habitat, agriculture, and similar uses [27, 29-30]. As natural and semi-natural habitats are continuously subjected to increasing pressure due to anthropogenic activities, monitoring the changes occurring in such areas has become a priority to ensure conservation and sustainable land use practices [31-35]. Quantifying the spatial and temporal patterns of LULC changes and their corresponding consequences is now recognized as a critical area of research in land change science [36].

Mining activities can significantly alter hydrological processes at various scales due to vegetation removal, canopy disruption, and modification of wetlands. The loss of vegetation cover and changes in soil infiltration capacity may considerably increase the flood generation potential of catchments, thereby leading to significant ecological consequences [20]. Furthermore, large-scale changes in surface materials can result in degrading of the natural landscape's aesthetic value [35]. The quantitative assessment of such LULC changes plays a crucial role in evaluating and managing the potential impacts of mining operations on natural systems. Among the various methods employed for monitoring open-pit mines, remote sensing-based LULC applications remain the most common and practical approach [37]. Today, various classification methods are used to investigate the temporal dynamics of LULC. In recent years, remote sensing scientists have increasingly adopted machine learning classification algorithms in LULC

mapping studies, as these methods have gained significant prominence in the processing of remote sensing data [38]. Machine learning techniques offer potential for the effective and efficient classification of satellite imagery [39-44]. Among the key strengths of machine learning are its ability to process high-dimensional data, map classes with highly complex characteristics, accept diverse input prediction variables, and operate without requiring assumptions about data distributions (i.e., non-parametric behavior) [41]. These techniques have become especially important in LULC mapping due to their capability to handle large volumes of multispectral satellite data with high accuracy and efficiency. Consequently, they are widely used as effective tools in environmental change analyses [41, 45-47]. Beyond improving the detection of subtle environmental changes, these methods also support timely decision-making in sustainable mining operations. Numerous studies conducted both globally and within Türkiye the setting of this research have demonstrated that machine learning methods facilitate more frequent updates and continuous monitoring in dynamic environments such as open-pit mining areas and generally yield high classification accuracies [48-53].

In this study, land use and land cover (LULC) changes in the Tunçbilek open-pit coal mine and its surrounding areas located within the borders of Tavşanlı district in Kütahya province were investigated using high-resolution PlanetScope imagery and supervised machine learning classification algorithms. The study focuses on detecting and analyzing the spatial and temporal surface changes caused by mining activities over five years. While numerous studies have explored LULC changes using remote sensing, limited research has mainly focused on the detailed analysis of the long-term environmental effects of open-pit coal mining in Türkiye using high-resolution PlanetScope satellite imagery combined with advanced machine learning techniques. This presents a significant scientific gap, particularly in the context of sustainable mining and environmental monitoring. By addressing this gap, the present study aims to demonstrate the effectiveness of this integrated approach in mapping and tracking mining-induced land cover transformations with high spatial detail, thereby contributing to the development of more accurate and timely monitoring frameworks for environmentally sensitive regions. Specifically, this study leverages the 3-meter-high spatial resolution of PlanetScope imagery to enable more precise detection of fine-scale surface changes caused by mining activities, offering an advantage over studies using medium-resolution data. Furthermore, by focusing on the Tunçbilek mining site, the research aims to provide an in-depth analysis of the regional environmental impacts, ultimately contributing valuable insights for the development of more effective monitoring systems and sustainable mining practices in similar ecological contexts.

## 2. Material and methods

Remote sensing (RS) and Geographic Information System (GIS) tools are widely utilized in the mining industry for various purposes, including mineral exploration, modeling and monitoring, mine planning and environmental

impact assessment [22-24]. The methodology of the present study is outlined in Figure 1, commencing with data acquisition and extending to the mapping of the LULC of the mine pit and its immediate surroundings using the MLC and SVM methods. Accuracy assessment was conducted afterwards to validate the classification outcomes and to ascertain which of the two classification mechanisms exhibited superior accuracy.

### 2.1 Study area

The Tunçbilek open-pit coal mine is located in the Tavşanlı district of Kütahya province, in the northern part of the Aegean region in Western Türkiye, approximately 62 km from the center of Kütahya (Figure 2). The region stands out due to its significant lignite reserves, playing a strategic role in providing energy for industry. Coal production in the Tunçbilek Basin began in 1924, and it was transferred to the Turkish Coal Enterprises (TKİ) in 1940. Today, coal production continues through both open-pit and underground mining methods, with approximately 80% of production coming from open-pit mining [27, 54].

The Tunçbilek mining site has undergone significant environmental pressures due to decades of mining activities, leading to changes in the region's ecological balance. The area surrounding the mine is a mixture of agricultural lands, forests, and settlements, making it essential to monitor the impacts of mining on the land use and land cover (LULC) over a wider geographical area. Furthermore, the fact that open-pit mining predominates in this site results in more pronounced environmental issues, such as surface deformation, vegetation loss, and the alteration of water resources.

In this context, the Tunçbilek mining site and its surrounding area were chosen for this study due to their high potential for monitoring environmental impacts, as well as the fact that this site has been an active and significant open-pit mining operation in Türkiye for many years. Additionally, the limited number of studies conducted in this area presents an opportunity to fill the gap in the literature, thereby enhancing the contributions of this research.

### 2.2 Data acquisition

To map, identify and evaluate the LULC in Tunçbilek Open Pit and its immediate vicinity, this study employs Planet Scope satellite imagery, which is distinguished by its significant divergence from conventional free satellite data due to its high resolution. Planet operates the largest fleet of Earth observation satellites, with a current total of 200 satellites in orbit. This extensive satellite network provides global coverage, offering high spatial and temporal resolution imagery [55-56]. The Planet Scope constellation presently encompasses three generations of remote sensing satellites: Dove Classic, Dove-R and SuperDoves. The Dove Classic, launched in 2016, carries a 4-band (RGB-NIR) 'PS2' sensor with a ground sampling distance (GSD) of approximately 3.7 m (Table 1).

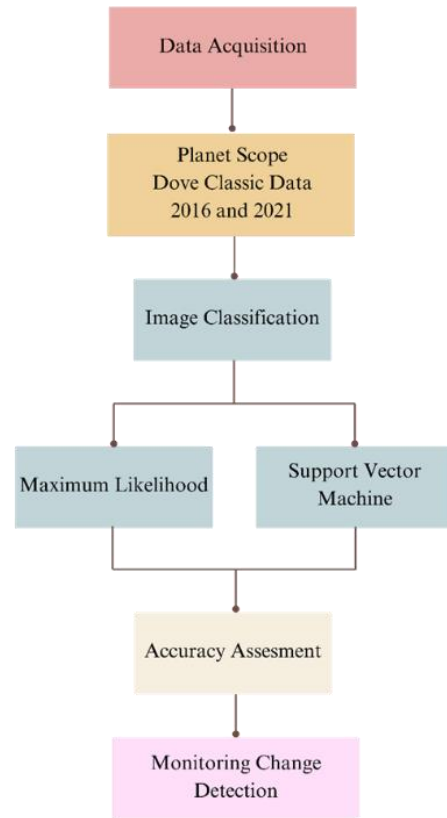


Figure 1. The following flowchart illustrates the general methodology employed in this study

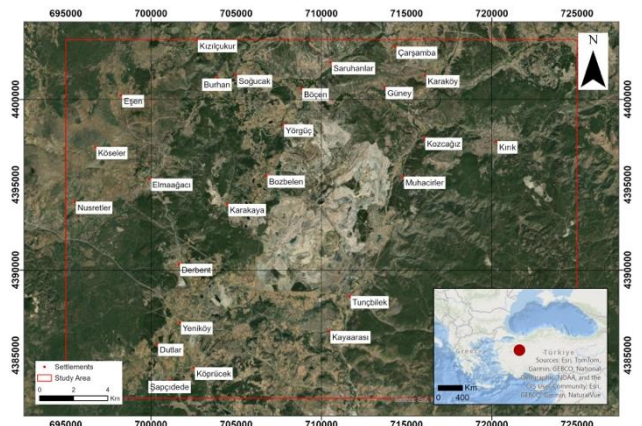
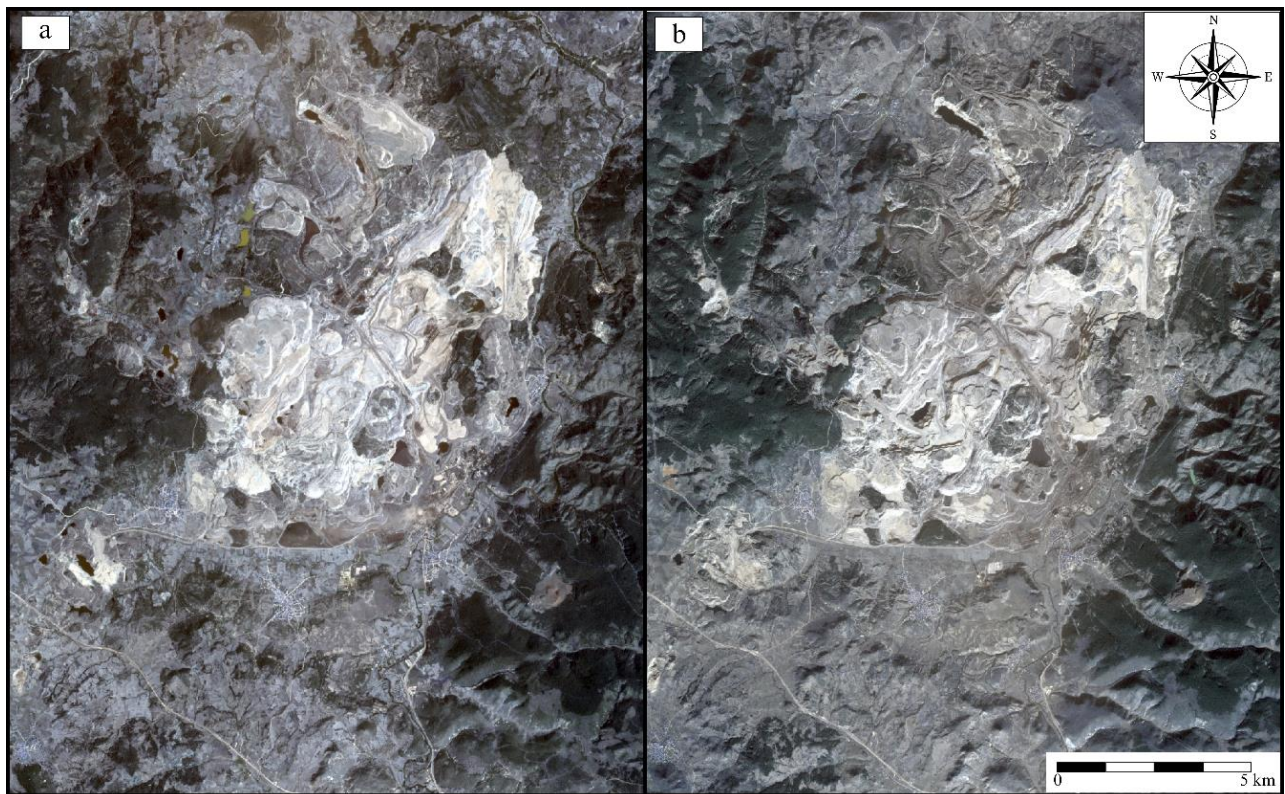


Figure 2. Generalized view of the study area and settlements around its vicinity

These data provided free of charge under an educational use license from Planet Lab Inc. website. Planet Scope satellite data are downloaded in a ready-to-use format in the form of quad-band images (Red, Green, Blue and Near infrared), i.e. without any pre-processing (Figure 3) [29, 56]. These characteristics make Planet Scope satellite data a unique resource for studying heterogeneous urban landscapes (Table 1).



**Figure 3.** True-color PlanetScope satellite images of the study area acquired in 2016 and 2021, generated using the standard RGB bands.

**Table 1.** Details of Planet Scope images used in the study

Year	Acquisition Date	Bands Used	Instrument	Spatial Resolution
2021	02/08/2021	Band 1(Blue, 455-515 nm), Band 2 (Green, 500-590 nm), Band 3 (Red, 590-670 nm), Band 4 (Near-Infrared, 780-860 nm)	Dove Classic	3 meters
2016	11/08/2016	Band 1(Blue, 455-515 nm), Band 2 (Green, 500-590 nm), Band 3 (Red, 590-670 nm), Band 4 (Near-Infrared, 780-860 nm)	Dove Classic	3 meters

### 2.3 Data processing

A four-step approach was used to analyze land use changes in the Tunçbilek Open Pit Coal Mine according to the workflow summarised in Figure 1. The flowchart includes data collection, image classification, accuracy analysis, and evaluation of changes in land use classes over the years. As part of Step 1, PlanetScope images taken half a decade apart from 2016 to 2021 were used, ensuring cloud cover was less than 5%. These images, with a spatial resolution of approximately 3 meters, cover the entire study area. Notably, PlanetScope imagery is delivered as Analysis Ready Data (ARD), having already undergone preprocessing steps such as orthorectification, radiometric calibration, and basic atmospheric correction. Therefore, no additional preprocessing steps were required before the analysis.

LULC classification was performed using ArcGIS Pro by defining training samples for each of the six land cover classes. The classification method employed both Maximum Likelihood Classification (MLC) and Support Vector Machine (SVM) algorithms. This step leveraged the

advanced classification tools and capabilities of ArcGIS Pro to optimise accuracy and efficiency, enabling accurate identification of land cover types and changes over time. The classified raster images were first converted to polygon format to facilitate the calculation of each land use area. This conversion allowed for more precise measurements and enabled the identification of specific land use changes over time. Statistical summaries of these changes were then generated, providing insight into the extent and nature of land use dynamics in the study area. In addition, centrally connected polygons were identified and included in the calculations and change analysis to distinguish the open pit mine from other land use features. This methodology allowed for accurate identification and reliable quantification of land use changes.

### 2.4 Supervised classification

This study employs the Maximum Likelihood Classification (MLC) and Support Vector Machine (SVM) techniques to detect land use and land cover (LULC) changes resulting from mining activities in and around the surface

mining area. MLC is a classical supervised classification algorithm that relies on the statistical distribution of spectral data and has been extensively applied in remote sensing studies, particularly for LULC mapping [57-59]. However, in complex and heterogeneous environments such as open-pit mining areas, spectral overlap between different land cover classes is highly probable, can affect classification accuracy.

To address such complexities, SVM has been introduced as an advanced machine learning algorithm capable of modeling non-linear decision boundaries. It offers strong generalization capabilities and high classification accuracy potential in high-dimensional datasets, such as multi-band satellite imagery. Therefore, this study applies both MLC as a fundamental benchmark and SVM to explore the advantages of machine learning approaches in this specific context.

In supervised image classification, all pixels in raster data are categorized into predefined classes based on spectral characteristics. Both MLC and SVM have been widely utilized for the classification of surface mining areas [22-24, 60-62], with SVM particularly demonstrating improved classification accuracy in various studies [44].

MLC is a widely used supervised classification method applied in the classification of remotely sensed data [63-64]. Training data in MLC is used to generate a class signature based on variance and covariance. The algorithm assumes a normal distribution of each class instance in the multidimensional space, where the number of dimensions is equal to the number of bands in the image [64]. The probability that a pixel belongs to a specific class is computed using the multivariate normal distribution, as shown in Equation (1).

$$D = \ln(a_c) - [0.5 * \ln(|Cov_c|)] - [0.5x(X - M_c)^T x(Cov_c^{-1})x(X - M_c)] \quad (1)$$

SVM, based on statistical learning theory, is one of the most advanced and highly accurate supervised machine learning techniques, such as object-oriented image classification and fuzzy classifiers [36-38]. SVM is effective in classifying high-dimensional data, making it suitable for complex datasets in land cover, vegetation, and urban studies [65-67]. SVM aims to build a model that predicts the target value of data occurrences in the test set given only their attributes.

The primary objective of SVM is to find an optimal hyperplane that separates classes with the maximum margin. SVM is a non-parametric classifier capable of handling both linearly and non-linearly separable data efficiently [68].

If the training dataset consists of  $k$  samples represented as  $\{(x_i, y_i)\}$ , where  $x_i \in \mathbb{R}^n$  and  $y_i \in \{-1, +1\}$ , the classes are said to be linearly separable if there exists a vector  $w$  and a scalar  $b$  such that the inequalities given in Equation (2) and Equation (3) define the optimal separating hyperplane.

$$(W \cdot x_i + b) \geq +1 \text{ overall training samples with } y_i = +1 \quad (2)$$

$$(W \cdot x_i + b) \leq -1 \text{ overall training samples with } y_i = -1 \quad (3)$$

In practical remote sensing applications, it is frequently observed that the available datasets are not always linearly separable. To address this complexity, SVM utilizes kernel functions to project the input data into a higher-dimensional feature space where linear separation becomes feasible. Among the various kernel functions commonly used such as linear, polynomial, sigmoid, and radial basis function (RBF) the RBF kernel is frequently preferred in land use/land cover (LULC) classification tasks due to its strong generalization ability and its effectiveness in handling complex, non-linear class boundaries. Previous studies have reported that the RBF kernel provides reliable and high classification accuracy in a variety of LULC applications [69-74]. For this reason, the RBF kernel was selected in this study. The RBF kernel is defined in Equation (4) as follows:

$$K(X_i, X_j) = \exp(-\gamma \|X_i - X_j\|^2) \quad (4)$$

The parameter  $\gamma$ , which is specific to the kernel, has been demonstrated to exert a significant influence on the outcome of a single training example. It is evident that a reduced  $\gamma$  value engenders a more refined decision boundary, whilst an augmented one facilitates more intricate separations. The performance of the SVM classifier is contingent on the selection of both  $\gamma$  and the regularization parameter  $C$ , which governs the trade-off between achieving a low training error and a large margin. To ensure optimal classification performance, these parameters were fine-tuned using a grid-search method with  $k$ -fold cross-validation. Grid-search aims to find the best performing parameter set by systematically testing different combinations of  $\gamma$  and  $C$  values within specified ranges. Cross-validation, on the other hand, allows us to estimate the generalization ability of the model by evaluating its performance on different subsets of the data. In the context of multi-class classification problems in this study, the one-against-one strategy was employed, whereby binary classifiers were trained between every possible pair of classes.

In supervised classification, training samples are used to identify each class based on user-defined criteria. This study chose the National Land Cover Database 2011 to identify land cover classes (Table 2) [74-76]. In this study, six land cover classes were selected from the NLCD2011 classification scheme based on their spatial prevalence in the study area and their spectral separability in the PlanetScope imagery. Classes such as wetlands, shrublands, and grasslands were excluded due to their limited representation within the study region and the potential for spectral confusion with other dominant classes at the 3-meter spatial resolution. The selected classes Mining site, Water, Developed, Barren, Forest, and Planted/Cultivated represent the most significant land cover types relevant to the scope and objectives of this study. The classified Planet Scope images are presented in Figure 4, respectively.

**Table 2.** Land classes and descriptions used in the study

No	Class Name	Description
1	Mining Site	The area where mining activities are carried out
2	Water	Surface water and artificial lakes within the mining site
3	Developed	Settlements and roads
4	Barren	Bare and barren land is not included in the forest class
5	Forest	Tree-covered areas
6	Planted	Arable land

### 2.5 Accuracy assessment and change detection

After land use classification, it is imperative to evaluate the accuracy and reliability of the classified images to detect and quantify any mapping or classification errors. Various techniques have been developed to evaluate the accuracy of such classifications [24, 77-79]. In this study, confusion matrix, which is a widely used accuracy assessment method, was used and overall (OA), producer (PA) and user accuracies (UA) and  $k$  coefficient values were calculated for different classes [80-83]. In this study, reference data containing 101 points for six land use classes were randomly generated using ArcGIS Pro software and the method was applied. The estimated and actual reference values of land use maps produced with MLC and SVM methods for the years 2016 and 2021 were compared. Ground truth reference data were derived through visual interpretation of high-resolution Google Earth imagery, which provided temporally corresponding scenes to the PlanetScope data. Reference points were selected based on clearly distinguishable land cover features and cross-checked with prior studies and official land use information to ensure consistency and accuracy. Change detection involves assessing the differences in land cover using images obtained from Planet Scope images on selected dates using the applied classification methods [84]. After spatial change classification, raster data were converted into polygons in ArcGIS to calculate the area covered by each class in the mining site and its vicinity in 2016 and 2021. Then, the change developed in the mining site and its vicinity was calculated and a spatial layer was created to visualize the differences between the two time periods (Figures 3-4).

The accuracy metrics were computed using the following equations Equation (5), (6), (7): The most common method of quantifying agreement is known as the 'one-against-one' (OA) approach. This is indicated by the percentage of pixels that will be correctly categorised. Overall Accuracy (OA) was calculated as:

$$OA = \left( \sum_{i=1}^q X_{ii}/N \right) \times 100 \quad (5)$$

In this formula, the total number of classes is represented by  $q$ , the total number of pixels by  $N$ , and the corrected classified pixels, i.e. the diagonal ones, by  $X_{ii}$ .

Producer Accuracy (PA) for each class  $i$  was calculated as

$$PA = (X_{ii}/N_{i+}) \times 100 \quad (6)$$

$$UA = (X_{ii}/N_{+i}) \times 100 \quad (7)$$

where  $N_{i+}$  is the marginal sum of the rows and  $N_{+i}$  is the marginal sum of the columns.

The  $k$  coefficient, expressed by Equation 8, is used to measure the ratio between the actual and predicted stochastic agreement when the classifier is random.

$$k = \frac{(N \sum_{i=1}^q X_{ii} - \sum_{i=1}^q N_{i+}N_{+i})}{(N^2 - \sum_{i=1}^q N_{i+}N_{+i})} \quad (8)$$

### 3. Results and discussion

In this study, two supervised classification methods were evaluated on the 2016 and 2021 datasets as shown in Figure 4 and given in Table 3, and six different land use classes were successfully determined using these techniques.

Firstly, the six distinct land use categories were successfully identified through the implementation of the MLC technique. A subsequent evaluation of the results obtained in both 2016 and 2021 revealed that in 2016, the forest class dominated the study area with 38.36%, while in 2021 barren class became the most dominant class with 35.38%. The mining site class accounted for 13.00% in 2016 and 12.17% in 2021. The distribution of all other land use classes is presented in Table 3. The visual interpretation of the outputs generated by the method revealed that it produced classification errors in both years, in the form of overestimation of agricultural land by confusing it with barren land and slopes within the mine. This error was attributed to the similar spectral reflectance of these classes.

**Table 3.** Land use and land cover change analysis between 2016 and 2021 based on svm and mlc classification techniques

Class Name	MLC (%)			SVM (%)		
	2016	2021	Change	2016	2021	Change
Mining Site	13.00	12.17	-0.83	13.06	14.45	1.39
Water	0.73	2.22	1.50	2.41	2.38	-0.04
Developed	3.34	1.37	-1.96	2.48	1.20	-1.28
Barren	28.44	35.38	6.94	25.20	17.29	-7.90
Forest	38.36	28.84	-9.52	39.36	40.36	1.00
Planted	16.13	20.00	3.87	17.49	24.31	6.83

When the classification results obtained with the SVM classification method are analyzed, it is seen that the forest class is the most dominant in the field with an area of 39.36% and 40.36% in both 2016 and 2021, respectively (Table 3 and Figure 4). In 2016, the area allocated to coal mining accounted for 13.06% of the total area, while in 2021, this figure increased by 18% over the five-year period, covering approximately 14.5% of the study area. The distribution of other land use classes, including wasteland, surface water, agricultural land and settlements, is presented in Table 3.

Visual interpretation of the classification results revealed higher classification accuracy with the SVM method compared to the MLC method. The inconsistency in classification success can be attributed to various factors such as image quality, image resolution, classification errors, software errors and handling errors. In order to check the accuracy of the maps created after the classification methods, the maps classified with the MLC and SVM methods created for the years 2016 and 2021 were subjected to accuracy analysis. In order to evaluate the accuracy of these classified maps in ArcGIS Pro, after the classification using all classifiers, user accuracy (UA) (also referred to as recall), producer accuracy (PA) (precision), and the  $k$  coefficient were calculated (Table 4). Although the water class offers variable accuracy percentages in terms of UA and PA for the SVM and MLC classifiers of the methods applied here, respectively, it offers the lowest values together with the developed class, while the forest class generally has the highest accuracy values. The situation experienced in water and forest land may probably be due to the lack of a clear spectral signal that expresses the developed class, which represents the construction areas, and therefore it seems to mix with the mining area slope areas in places. Wetlands, on the other hand, gave low values in accuracy due to the reflections they make and the areas similar to the slopes of the mountains in places. In addition, the  $k$  coefficient used in the cluster analysis was also calculated. The  $k$  coefficient is used to measure the ratio between the actual and predicted stochastic agreement if the classifier is random.

When the classification results obtained with the SVM classification method are analyzed, it is seen that the forest class is the most dominant class in the field with an area of 39.36% and 40.36% in both 2016 and 2021, respectively (Table 3 and Figure 4). In 2016, the area allocated to coal mining accounted for 13.06% of the total area, while in 2021, this figure increased by 18% over the five-year period, covering approximately 14.5% of the study area. The distribution of other land use classes, including wasteland,

surface water, agricultural land and settlements, is presented in Table 3.

Visual interpretation of the classification results revealed higher classification accuracy with the SVM method compared to the MLC method. The inconsistency in classification success can be attributed to various factors such as image quality, image resolution, classification errors, software errors and handling errors. In order to check the accuracy of the maps created after the classification methods, the maps classified with the MLC and SVM methods created for the years 2016 and 2021 were subjected to accuracy analysis. In order to evaluate the accuracy of these classified maps in ArcGIS Pro, after the classification using all classifiers, overall accuracy (OA), user accuracy (UA) (also referred to as recall), producer accuracy (PA) (precision), and the  $k$  coefficient were calculated (Table 4, 5). Although the water class offers variable accuracy percentages in terms of UA and PA for the SVM and MLC classifiers of the methods applied here, respectively, it offers the lowest values together with the developed class, while the forest class generally has the highest accuracy values. The situation experienced in water and forest land may probably be due to the lack of a clear spectral signal that expresses the developed class, which represents the construction areas, and therefore it seems to mix with the mining area slope areas in places. Wetlands, on the other hand, gave low values in accuracy due to the reflections they make and the areas similar to the slopes of the mountains in places. In addition, the  $k$  coefficient used in the cluster analysis was also calculated. The  $k$  coefficient is used to measure the ratio between the actual and predicted stochastic agreement if the classifier is random.

The  $k$  coefficient is categorized as shown. The meanings of the kappa values ranging from -1 to 1 are given in (Table 6) [85]. According to the results obtained, the SVM classifier surpassed the MLC by providing higher classification accuracy for each class. The kappa value for MLC was determined as 0.73 in 2016 and 0.72 in 2021, and for SVM, it was determined as 0.87 in 2016 and 0.84 in 2021.

**Table 4.** Accuracy assessment using confusion matrix generated from test training samples for Planet Scope Dove Classic images based on MLC and SVM techniques

Class Name	2016				2021			
	MLC		SVM		MLC		SVM	
	User's Accuracy %	Producer's Accuracy %						
Mining Site	80	60	100	82.25	59.09	86.66	85.71	85.71
Water	60	100	100	100	80	100	40	100
Developed	50	71.43	60	100	44.44	57.14	60	85.72
Barren	63.75	66.66	100	78.12	76.19	61.53	100	89.47
Forest	97.14	94.44	100	100	100	92.1	97.5	90.7
Planted	84	77.77	52.94	90	77.59	77.59	95.83	85.19

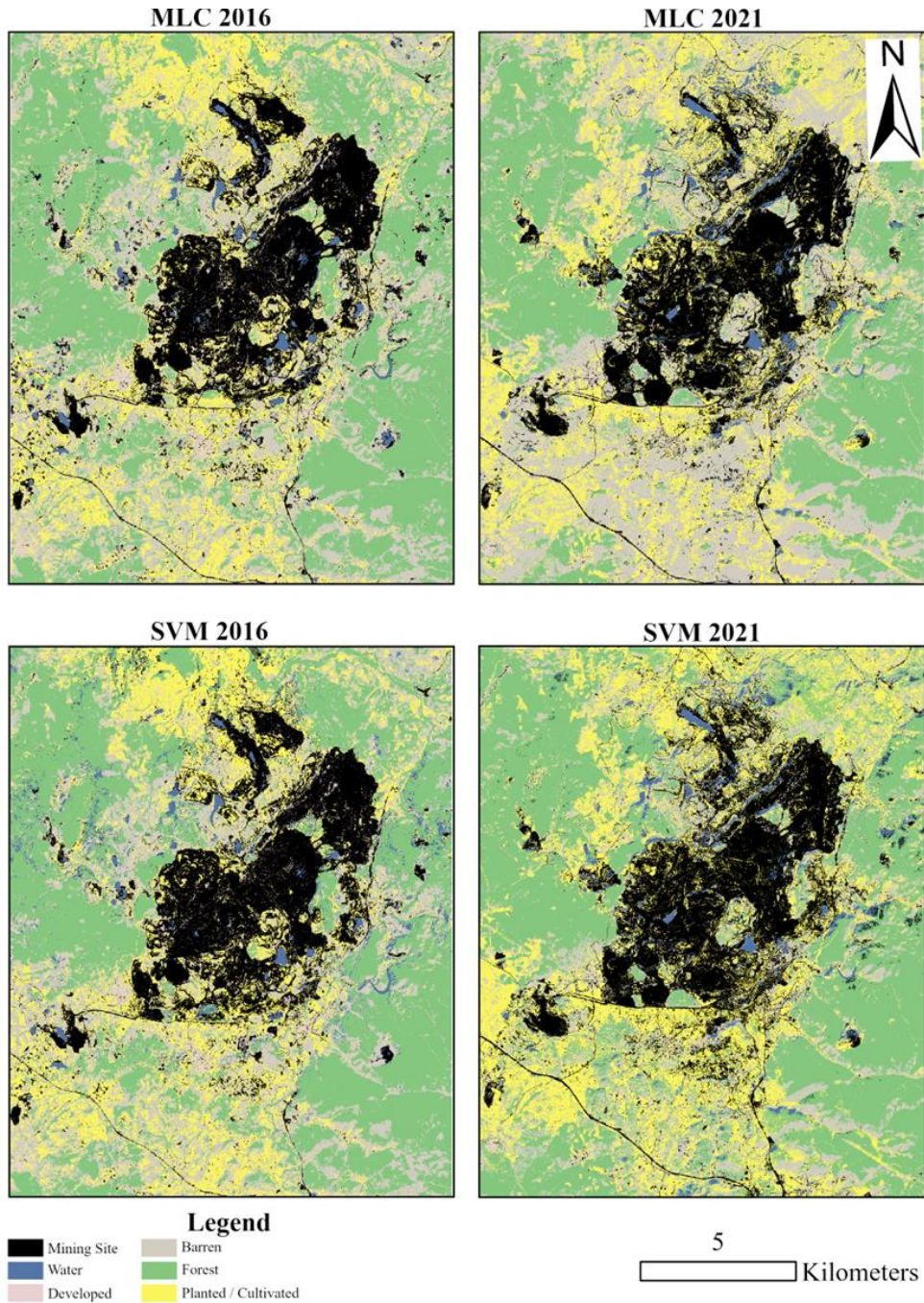


**Figure 4.** Land cover change map of the study area from 2016 to 2021

**Table 5.** Overall Accuracy and Kappa Statistics for 2016 and 2021 Classifications

Year	MLC		SVM	
	Overall Accuracy %	<i>k</i> Coefficient	Overall Accuracy %	<i>k</i> Coefficient
2016	79	0.73	89	0.84
2021	78	0.72	87	0.87

It is seen that there is a difference of approximately 10% between the two methods. It is seen that SVM is in the "very good" range because it remains between 0.81 and 1, while for MLC, although the values are low, they remain between

the "good" range of 0.61 and 0.80. In this study, SVM not only outperformed MLC in classifying all linearly separable classes but also achieved superior results when training classes with different spectral reflectance(s).

As a result of the accuracy assessment, images classified by SVM reported higher accuracy for both 2006 and 2016, so images classified by SVM were used to detect changes after classification over the years. According to the results obtained, there was an increase in the mining site, forest and agricultural land classes and a decrease in the water, residential areas and barren land class in 2021 compared to 2016. While the most significant decrease among land

classes was experienced in barren land, the greatest increase occurred in agricultural lands (Table 7).

**Table 6.** *k* Coefficient Values and Interpretation

Interpretation	Value Range
Very Good	0.81 - 1.00
Good	0.61 - 0.80
Moderate	0.41 - 0.60
Fair	0.21 - 0.40
Poor	-1.00 - 0.20

**Table 7.** Land cover changes Tunçbilek mining site and its vicinity (hectare(ha))

Class Name	2016		2021		2021-2016 Change (%)
	hectar (ha)	%	hectar (ha)	%	
Mining Site	4309.27	13.06	4973.38	14.45	1.39
Water	796.39	2.41	818.03	2.38	-0.04
Developed	816.83	2.48	412.91	1.20	-1.28
Barren	8310.90	25.20	5950.32	17.29	-7.90
Forest	12982.24	39.36	13888.59	40.36	1.00
Planted	5767.96	17.49	8366.08	24.31	6.83

These changes may have occurred as a result of the interaction between various anthropogenic and environmental factors. The observed increase in cultivated areas (+6.83%) could be associated with local land conversion initiatives or a rising demand for agricultural production in response to socioeconomic pressures. The noticeable decrease in barren land (-7.90%) might be related to land rehabilitation efforts, afforestation activities, or the expansion of agricultural use into previously unused areas. The slight increase in forest cover (+1.00%) could be explained by natural regeneration processes or potential afforestation programs, particularly in less disturbed regions. The reduction in developed areas (-1.28%) may reflect the relocation of settlements or abandonment of minor built-up zones due to the expansion of mining operations. These spatial change patterns reflect a complex interplay between human activities and ecological processes in the Tunçbilek mining region. In future studies, these drivers could be explored in greater detail by integrating socioeconomic data and field-based observations.

#### 4. Conclusion and Suggestions

In our study, the land use/land cover (LULC) changes that occurred within a short period (five years) over a relatively small area (approximately 35 hectares) in the Tavşanlı district of Kütahya, western Türkiye a region known for intensive mining activity were investigated using remote sensing methods. Unlike many comparable studies in the literature that rely on freely available medium-resolution satellite data (e.g., Landsat, Sentinel), this study employed high-resolution PlanetScope imagery (3 m), which enhanced image sharpness, facilitated the selection of training points, and contributed to higher classification accuracy.

Similar to the findings of [47, 86-89] our results show that Support Vector Machine (SVM) performs better than Maximum Likelihood Classification (MLC), particularly in cases where land cover classes exhibit overlapping spectral characteristics. Confusion matrix-based accuracy assessment revealed that SVM yielded higher overall accuracy and outperformed MLC in classifying individual categories such as forest and cultivated land, consistent with previous comparative studies in heterogeneous landscapes.

Moreover, this study provides a more localized perspective by applying machine learning techniques to a small-scale mining site. It demonstrates the applicability of these methods in limited geographic extents with reduced computational demands, making them practical for rapid land cover monitoring. While many previous studies have examined land cover dynamics over large regions using medium-resolution imagery, our approach highlights the potential for detailed temporal analysis using very high-resolution satellite data (3 m), which is particularly suitable for monitoring land cover change in small-scale surface mining areas.

According to our findings, a ~1.5% expansion in mining land was observed, while the dominant land cover class (forest) remained stable, indicating limited encroachment into ecologically sensitive zones. These findings can inform local-scale reclamation planning, and the methodological framework can be extended to other sites with similar characteristics.

In conclusion, this study complements and extends previous research by showcasing how the integration of high-resolution satellite imagery with advanced classification methods like SVM offers a reliable, repeatable, and scalable approach for monitoring land use dynamics, particularly in regions undergoing rapid landscape transformation due to mining. Future research could further enhance this methodology by integrating different data sources (e.g., multi-temporal images, radar, or hyperspectral data) and exploring alternative machine learning algorithms to achieve a more comprehensive understanding of land cover changes and improve classification robustness for environmental monitoring in mining areas.

#### Acknowledgement

The authors would like to express their sincere gratitude to Planet Labs for providing free access to high-resolution PlanetScope satellite imagery, which was instrumental for the analysis conducted in this study. Their support in facilitating open access to Earth observation data is highly appreciated and significantly contributes to the advancement of environmental monitoring and academic research.

#### Conflict of Interest

The authors declare no conflict of interest.

#### Similarity ratio (iThenticate): % 18

#### References

- [1] K. Barış and S. Küçükali, Availability of renewable energy sources in Turkey: Current situation, potential, government policies and the EU perspective, Energy

- Policy, vol. 42, pp. 377–391, 2012, <https://doi.org/10.1016/j.enpol.2011.12.002>.
- [2] Y. Huang, S. M. F. Raza, I. Hanif, M. Alharthi, Q. Abbas, and S. Zain-ul-Abidin, The role of forest resources, mineral resources, and oil extraction in economic progress of developing Asian economies, *Resources Policy*, vol. 69, p. 101878, 2020, <https://doi.org/10.1016/j.resourpol.2020.101878>.
- [3] A. E. Patiño Douce, Metallic Mineral Resources in the Twenty-First Century. I. Historical Extraction Trends and Expected Demand, *Natural Resources Research*, vol. 25, no. 1, pp. 71–90, 2016, <https://doi.org/10.1007/s11053-015-9266-z>.
- [4] M. M. Poulton, S. C. Jagers, S. Linde, D. Van Zyl, L. J. Danielson, and S. Matti, State of the World's Nonfuel Mineral Resources: Supply, Demand, and Socio-Institutional Fundamentals, *Annu Rev Environ Resour*, vol. 38, no. 1, pp. 345–371, 2013, <https://doi.org/10.1146/annurev-environ-022310-094734>.
- [5] O. Vidal, H. Le Boulzec, B. Andrieu, and F. Verzier, Modelling the Demand and Access of Mineral Resources in a Changing World, *Sustainability*, vol. 14, no.1, p.11, 2021, <https://doi.org/10.3390/su14010011>.
- [6] K. Barış, The role of coal in energy policy and sustainable development of Turkey: Is it compatible to the EU energy policy?, *Energy Policy*, vol. 39, no. 3, pp. 1754–1763, Mar. 2011, <https://doi.org/10.1016/j.enpol.2011.01.007>.
- [7] Y. Kasap, C. Şensöğüt, and Ö. Ören, Efficiency change of coal used for energy production in Turkey, *Resources Policy*, vol. 65, p. 101577, 2020, <https://doi.org/10.1016/j.resourpol.2019.101577>.
- [8] Y. Kasap and F. Duman, Use Efficiency of Primary Energy Resources in Turkey, *Energy Exploration & Exploitation*, vol. 31, no. 6, pp. 937–952, 2013, <https://doi.org/10.1260/0144-5987.31.6.937>.
- [9] M. S. Delibalta, Türkiye madencilik sektöründe dögüsel ekonomi ve dijitalleşme uygulamaları, *Ömer Halisdemir Üniversitesi Mühendislik Bilimleri Dergisi*, 2022, <https://doi.org/10.28948/ngumuh.1141644>.
- [10] M. S. DELİBALTA, Türkiye kömür rezervlerinin rasyonel değerlendirilmesi ve ekonomik önemi, *Ömer Halisdemir Üniversitesi Mühendislik Bilimleri Dergisi*, 2024, <https://doi.org/10.28948/ngumuh.1391184>.
- [11] Y. Shan, L. Čuček, P. S. Varbanov, J. J. Klemeš, K. Pan, and H. Zhu, Footprints Evaluation of China's Coal Supply Chains, *Computer Aided Chemical Engineering*, vol. 33, pp. 1879–1884, Jan. 2014, <https://doi.org/10.1016/B978-0-444-63455-9.50148-3>.
- [12] R. D. Singh, Principles and Practices of Modern Coal Mining. New Age Publishing, 2005.
- [13] J. (Jim) Zhang and K. R. Smith, Household Air Pollution from Coal and Biomass Fuels in China: Measurements, Health Impacts, and Interventions, *Environ Health Perspect*, vol. 115, no. 6, pp. 848–855, 2007, <https://doi.org/10.1289/ehp.9479>.
- [14] J. Chang-sheng, C. Zhao-xue, and C. Qing-hua, Surface coal mining practice in China, *Procedia Earth and Planetary Science*, vol. 1, no. 1, pp. 76–80, 2009, <https://doi.org/10.1016/j.proeps.2009.09.014>.
- [15] D. B. Gesch, Analysis of Multi-Temporal Geospatial Data Sets to Assess the Landscape Effects of Surface Mining, *Journal American Society of Mining and Reclamation*, vol. 2005, no. 1, pp. 415–432, 2005, <https://doi.org/10.21000/JASMR05010415>.
- [16] Z. Li, Z. Ma, T. J. van der Kuijp, Z. Yuan, and L. Huang, A review of soil heavy metal pollution from mines in China: Pollution and health risk assessment, *Science of The Total Environment*, vol. 468–469, pp. 843–853, 2014, <https://doi.org/10.1016/j.scitotenv.2013.08.090>.
- [17] D. Ruppen, J. Runnalls, R. M. Tshimanga, B. Wehrli, and D. Odermatt, Optical remote sensing of large-scale water pollution in Angola and DR Congo caused by the Catoca mine tailings spill, *International Journal of Applied Earth Observation and Geoinformation*, vol. 118, p. 103237, 2023, <https://doi.org/10.1016/j.jag.2023.103237>.
- [18] V. Schueler, T. Kuemmerle, and H. Schröder, Impacts of Surface Gold Mining on Land Use Systems in Western Ghana, *Ambio*, vol. 40, no. 5, pp. 528–539, 2011, <https://doi.org/10.1007/s13280-011-0141-9>.
- [19] R. N. Sousa and M. M. Veiga, Using Performance Indicators to Evaluate an Environmental Education Program in Artisanal Gold Mining Communities in the Brazilian Amazon, *AMBIO: A Journal of the Human Environment*, vol. 38, no. 1, pp. 40–46, 2009, <https://doi.org/10.1579/0044-7447-38.1.40>.
- [20] P. A. Townsend, D. P. Helmers, C. C. Kingdon, B. E. McNeil, K. M. de Beurs, and K. N. Eshleman, Changes in the extent of surface mining and reclamation in the Central Appalachians detected using a 1976–2006 Landsat time series, *Remote Sens Environ*, vol. 113, no. 1, pp. 62–72, 2009, <https://doi.org/10.1016/j.rse.2008.08.012>.
- [21] M. Hendrychová and M. Kabrna, An analysis of 200-year-long changes in a landscape affected by large-scale surface coal mining: History, present and future, *Applied Geography*, vol. 74, pp. 151–159, 2016, <https://doi.org/10.1016/j.apgeog.2016.07.009>.
- [22] N. Demirel, M. K. Emil, and H. S. Duzgun, Surface coal mine area monitoring using multi-temporal high-resolution satellite imagery, *Int J Coal Geol*, vol. 86, no. 1, pp. 3–11, 2011, <https://doi.org/10.1016/j.coal.2010.11.010>.
- [23] W. Pei et al., Mapping and detection of land use change in a coal mining area using object-based image analysis, *Environ Earth Sci*, vol. 76, no. 3, 2017, <https://doi.org/10.1007/s12665-017-6444-9>.
- [24] S. K. Karan and S. R. Samadder, Accuracy of land use change detection using support vector machine and maximum likelihood techniques for open-cast coal

- mining areas, *Environ Monit Assess*, vol. 188, no. 8, 2016, <https://doi.org/10.1007/s10661-016-5494-x>.
- [25] S. Y. Çiçekli, Comparison of object based and pixel based classification methods in land use and land cover determination studies: The case of Yedigöze Reservoir Area, *Bilim. Derg. / NOHU J. Eng. Sci.*, vol. 13, no. 4, pp. 1372–1381, 2024, <https://doi.org/10.28948/ngmuh.1472869>.
- [26] M. Allam, N. Bakr, and W. Elbably, Multi-temporal assessment of land use/land cover change in arid region based on landsat satellite imagery: Case study in Fayoum Region, Egypt, *Remote Sens Appl.*, vol. 14, pp. 8–19, 2019, <https://doi.org/10.1016/j.rsase.2019.02.002>.
- [27] R. Mahmoud, M. Hassanin, H. Al Feel, and R. M. Badry, Machine Learning-Based Land Use and Land Cover Mapping Using Multi-Spectral Satellite Imagery: A Case Study in Egypt, *Sustainability (Switzerland)*, vol. 15, no. 12, 2023, <https://doi.org/10.3390/su15129467>.
- [28] C. M. Viana, S. Oliveira, S. C. Oliveira, and J. Rocha, Land Use/Land Cover Change Detection and Urban Sprawl Analysis, in *Spatial Modeling in GIS and R for Earth and Environmental Sciences*, Elsevier, 2019, pp. 621–651. <https://doi.org/10.1016/B978-0-12-815226-3.00029-6>.
- [29] C. Marais Sicre, R. Fieuzal, and F. Baup, Contribution of multispectral (optical and radar) satellite images to the classification of agricultural surfaces, *International Journal of Applied Earth Observation and Geoinformation*, vol. 84, p. 101972, 2020, <https://doi.org/10.1016/j.jag.2019.101972>.
- [30] C. Zhang et al., Improved Remote Sensing Image Classification Based on Multi-Scale Feature Fusion, *Remote Sens (Basel)*, vol. 12, no. 2, p. 213, 2020, <https://doi.org/10.3390/rs12020213>.
- [31] E. K. Antwi, R. Krawczynski, and G. Wiegler, Detecting the effect of disturbance on habitat diversity and land cover change in a post-mining area using GIS, *Landsc Urban Plan.*, vol. 87, no. 1, pp. 22–32, 2008, <https://doi.org/10.1016/j.landurbplan.2008.03.009>.
- [32] J. Belmaker et al., Empirical evidence for the scale dependence of biotic interactions, *Global Ecology and Biogeography*, vol. 24, no. 7, pp. 750–761, Jul. 2015, <https://doi.org/10.1111/geb.12311>.
- [33] R. Latifovic, K. Fytas, J. Chen, and J. Paraszczak, Assessing land cover change resulting from large surface mining development, *International Journal of Applied Earth Observation and Geoinformation*, vol. 7, no. 1, pp. 29–48, May 2005, <https://doi.org/10.1016/j.jag.2004.11.003>.
- [34] R. V. O'Neill et al., Monitoring Environmental Quality at the Landscape Scale, *Bioscience*, vol. 47, no. 8, pp. 513–519, 1997, <https://doi.org/10.2307/1313119>.
- [35] G. P. Petropoulos, P. Partsinevelos, and Z. Mitraka, Change detection of surface mining activity and reclamation based on a machine learning approach of multi-temporal Landsat TM imagery, *Geocarto Int.*, vol. 28, no. 4, pp. 323–342, 2013, <https://doi.org/10.1080/10106049.2012.706648>.
- [36] C. Zhang, P. A. Harrison, X. Pan, H. Li, I. Sargent, and P. M. Atkinson, Scale Sequence Joint Deep Learning (SS-JDL) for land use and land cover classification, *Remote Sens Environ.*, vol. 237, p. 111593, 2020, <https://doi.org/10.1016/j.rse.2019.111593>.
- [37] L. Yu et al., Monitoring surface mining belts using multiple remote sensing datasets: A global perspective, *Ore Geol Rev.*, vol. 101, pp. 675–687, Oct. 2018, <https://doi.org/10.1016/j.oregeorev.2018.08.019>.
- [38] H. Shih, D. A. Stow, and Y. H. Tsai, Guidance on and comparison of machine learning classifiers for Landsat-based land cover and land use mapping, *Int J Remote Sens.*, vol. 40, no. 4, pp. 1248–1274, 2019, <https://doi.org/10.1080/01431161.2018.1524179>.
- [39] M. G. Gumus and S. S. Durduran, The performance analyses of support vector machine classifiers for examination of the temporal change of land-use/cover in the Beyşehir Basin in Turkey (1984-2018), *Journal of Geodesy and Geoinformation*, vol. 8, no. 1, pp. 57–71, May 2021, <https://doi.org/10.9733/JGG.2021R0005.E>.
- [40] C. Huang, L. S. Davis, and J. R. G. Townshend, An assessment of support vector machines for land cover classification, *Int J Remote Sens.*, vol. 23, no. 4, pp. 725–749, 2002, <https://doi.org/10.1080/01431160110040323>.
- [41] A. E. Maxwell, T. A. Warner, and F. Fang, Implementation of machine-learning classification in remote sensing: an applied review, *Int J Remote Sens.*, vol. 39, no. 9, pp. 2784–2817, 2018, <https://doi.org/10.1080/01431161.2018.1433343>.
- [42] G. Mountrakis, J. Im, and C. Ogole, Support vector machines in remote sensing: A review, *ISPRS Journal of Photogrammetry and Remote Sensing*, vol. 66, no. 3, pp. 247–259, 2011, <https://doi.org/10.1016/j.isprsjprs.2010.11.001>.
- [43] M. Pal, Random forest classifier for remote sensing classification, *Int J Remote Sens.*, vol. 26, no. 1, pp. 217–222, 2005, <https://doi.org/10.1080/01431160412331269698>.
- [44] M. Pal and P. M. Mather, Support vector machines for classification in remote sensing, *Int J Remote Sens.*, vol. 26, no. 5, pp. 1007–1011, 2005, <https://doi.org/10.1080/01431160512331314083>.
- [45] A. M. Abdi, Land cover and land use classification performance of machine learning algorithms in a boreal landscape using Sentinel-2 data, *GISci Remote Sens.*, vol. 57, no. 1, pp. 1–20, 2020, <https://doi.org/10.1080/15481603.2019.1650447>.
- [46] B. Ghimire, J. Rogan, V. Galiano, P. Panday, and N. Neeti, An evaluation of bagging, boosting, and random forests for land-cover classification in Cape Cod, Massachusetts, USA, *GISci Remote Sens.*, vol. 49, no. 5, pp. 623–643, 2012, <https://doi.org/10.2747/1548-1603.49.5.623>.

- [47] C. Huang, L. S. Davis, and J. R. G. Townshend, An assessment of support vector machines for land cover classification, *Int J Remote Sens*, vol. 23, no. 4, pp. 725–749, 2002, <https://doi.org/10.1080/01431160110040323>.
- [48] D. D. Gbedzi et al., Impact of mining on land use land cover change and water quality in the Asutifi North District of Ghana, West Africa, *Environmental Challenges*, vol. 6, p. 100441, 2022, <https://doi.org/10.1016/j.envc.2022.100441>.
- [49] M. Siljander, Land use/land cover classification for the iron mining site of Kishushe, Kenya: A feasibility study of traditional and machine learning algorithms, 2020.
- [50] S. Vlachogianni, A. Servou, K. Karalidis, N. Paraskevis, M. Menegaki, and C. Roumpos, Remote sensing-based monitoring of land use and cover dynamics in surface lignite mining regions: a supervised classification approach, *Earth Sci Inform*, vol. 18, no. 2, p. 256, 2025, <https://doi.org/10.1007/s12145-025-01781-5>.
- [51] I. Vorovencii, Long-term land cover changes assessment in the Jiului Valley mining basin in Romania, *Front Environ Sci*, vol. 12, 2024, <https://doi.org/10.3389/fenvs.2024.1320009>.
- [52] M. Zhang, W. Zhou, and Y. Li, The analysis of object-based change detection in mining area: A case study with Pingshuo coal mine, in *International Archives of the Photogrammetry, Remote Sensing and Spatial Information Sciences - ISPRS Archives*, International Society for Photogrammetry and Remote Sensing, 2017. <https://doi.org/10.5194/isprs-archives-XLII-2-W7-1017-2017>.
- [53] M. Zhang, J. Wang, and Y. Feng, Temporal and spatial change of land use in a large-scale opencast coal mine area: A complex network approach, *Land use policy*, vol. 86, pp. 375–386, 2019, <https://doi.org/10.1016/j.landusepol.2019.05.020>.
- [54] Garp Lignite Operations Directorate, Faaliyetler. <https://gli.tki.gov.tr/faaliyetler>, Accessed 13 May 2025.
- [55] Planet Imagery Product Specifications, Planet Imagery Product Specifications. <https://assets.planet.com/docs/combined-imagery-product-spec-april-2019.pdf> Accessed 08 March 2025.
- [56] B. E. Lefulebe, A. Van der Walt, and S. Xulu, Fine-Scale Classification of Urban Land Use and Land Cover with PlanetScope Imagery and Machine Learning Strategies in the City of Cape Town, South Africa, *Sustainability*, vol. 14, no. 15, p. 9139, Jul. 2022, <https://doi.org/10.3390/su14159139>.
- [57] M. Xu, P. Watanachaturaporn, P. Varshney, and M. Arora, Decision tree regression for soft classification of remote sensing data, *Remote Sens Environ*, vol. 97, no. 3, pp. 322–336, 2005, <https://doi.org/10.1016/j.rse.2005.05.008>.
- [58] K. S. Rawat, S. Kumar, and N. Garg, Statistical comparison of simple and machine learning based land use and land cover classification algorithms: A case study, *Journal of Water Management Modeling*, 2024, <https://doi.org/10.14796/JWMM.H524>.
- [59] P. K. Srivastava, D. Han, M. A. Rico-Ramirez, M. Bray, and T. Islam, Selection of classification techniques for land use/land cover change investigation, *Advances in Space Research*, vol. 50, no. 9, pp. 1250–1265, 2012, <https://doi.org/10.1016/j.asr.2012.06.032>.
- [60] M. Ustuner, F. B. Sanli, and B. Dixon, Application of Support Vector Machines for Landuse Classification Using High-Resolution RapidEye Images: A Sensitivity Analysis, *Eur J Remote Sens*, vol. 48, no. 1, pp. 403–422, 2015, <https://doi.org/10.5721/EuJRS20154823>.
- [61] D. Gülçin, Arazi Kullanımının Sınıflandırılmasında Pikel ve Obje Tabanlı Sınıflandırmanın Karşılaştırılması, *Adnan Menderes Üniversitesi Ziraat Fakültesi Dergisi*, vol. 15, no. 2, pp. 43–49, 2018, <https://doi.org/10.25308/aduziraat.423782>.
- [62] J. D. DeWitt, P. G. Chirico, S. E. Bergstresser, and T. A. Warner, Multi-scale 46-year remote sensing change detection of diamond mining and land cover in a conflict and post-conflict setting, *Remote Sens Appl*, vol. 8, pp. 126–139, 2017, <https://doi.org/10.1016/j.rsase.2017.08.002>.
- [63] O. HAGNER and H. REESE, A method for calibrated maximum likelihood classification of forest types, *Remote Sens Environ*, vol. 110, no. 4, pp. 438–444, 2007, <https://doi.org/10.1016/j.rse.2006.08.017>.
- [64] J. A. Richards, Clustering and Unsupervised Classification, in *Remote Sensing Digital Image Analysis*, Berlin, Heidelberg: Springer Berlin Heidelberg, pp. 319–341., 2013, [https://doi.org/10.1007/978-3-642-30062-2\\_9](https://doi.org/10.1007/978-3-642-30062-2_9).
- [65] S. Y. Çiçekli, Arazi Kullanımı ve Arazi Örtüsü Belirleme Çalışmalarında Sınıflandırma Yöntemlerinin Karşılaştırılması: Yedigöze Baraj Gölü ve Çevresi Örneği, *Ömer Halisdemir Üniversitesi Mühendislik Bilimleri Dergisi*, 2024, <https://doi.org/10.28948/ngumuh.1472869>.
- [66] B. F. Noble, Environmental Impact Assessment, in *Encyclopedia of Life Sciences*, Wiley, 2011. <https://doi.org/10.1002/9780470015902.a0003253.pu.b2>.
- [67] D. A. Pisner and D. M. Schnyer, Support vector machine, in *Machine Learning*, Elsevier, pp. 101–121, 2020. <https://doi.org/10.1016/B978-0-12-815739-8.00006-7>.
- [68] V. N. Vapnik and A. Y. Chervonenkis, On the Uniform Convergence of the Frequencies of Occurrence of Events to Their Probabilities, in *Empirical Inference*, Berlin, Heidelberg: Springer Berlin Heidelberg, pp. 7–12, 2013., [https://doi.org/10.1007/978-3-642-41136-6\\_2](https://doi.org/10.1007/978-3-642-41136-6_2).
- [69] H. Tamirat, M. Argaw, and M. Tekalign, Support vector machine-based spatiotemporal land use land cover change analysis in a complex urban and rural

- landscape of Akaki river catchment, a Suburb of Addis Ababa, Ethiopia, *Heliyon*, vol. 9, no. 11, 2023, <https://doi.org/10.1016/j.heliyon.2023.e22510>.
- [70] G. Mountrakis, J. Im, and C. Ogole, Support vector machines in remote sensing: A review, *ISPRS Journal of Photogrammetry and Remote Sensing*, vol. 66, no. 3, pp. 247–259, 2011, <https://doi.org/10.1016/j.isprsjprs.2010.11.001>.
- [71] S. Martins, N. Bernardo, I. Ogashawara, and E. Alcantara, Support Vector Machine algorithm optimal parameterization for change detection mapping in Funil Hydroelectric Reservoir (Rio de Janeiro State, Brazil), *Model Earth Syst Environ*, vol. 2, no. 3, p. 138, 2016, <https://doi.org/10.1007/s40808-016-0190-y>.
- [72] C. Avcı, M. Budak, N. Yağmur, And F. Balçık, Comparison between random forest and support vector machine algorithms for LULC classification, *International Journal of Engineering and Geosciences*, vol. 8, no. 1, pp. 1–10, 2023, <https://doi.org/10.26833/ijeg.987605>.
- [73] S. R. Borra, S. A. V, Z. Alsalamı, Y. Chanti, and G. Ramesh, Support Vector Machine with Linear and Radial Bias Function to Classify the Soil Erosion and Land Degradation, in 2024 International Conference on Distributed Systems, Computer Networks and Cybersecurity (ICDSCNC), IEEE, Sep. pp. 1–5, 2024., <https://doi.org/10.1109/ICDSCNC62492.2024.10940051>.
- [74] T. Kavzoğlu and I. Çölkesen, A kernel functions analysis for support vector machines for land cover classification, *International Journal of Applied Earth Observation and Geoinformation*, vol. 11, no. 5, pp. 352–359, 2009, <https://doi.org/10.1016/j.jag.2009.06.002>.
- [75] C. Homer and L. Yang, Completion of the 2011 National Land Cover Database for the Conterminous United States-Representing a Decade of Land Cover Change Information, <https://doi.org/10.14358/PERS.81.5.345>.
- [76] J. Wickham, S. V. Stehman, D. G. Sorenson, L. Gass, and J. A. Dewitz, Thematic accuracy assessment of the NLCD 2019 land cover for the conterminous United States, *GIsci Remote Sens*, vol. 60, no. 1, 2023, <https://doi.org/10.1080/15481603.2023.2181143>.
- [77] S. Aronoff, Classification Accuracy: A User Approach.
- [78] George, Rosenfield, and K. Fitzpatrick-Lins, A coefficient of agreement as a measure of thematic classification accuracy., *Photogramm Eng Remote Sensing*, vol. 52, pp. 223–227, 1986.
- [79] S. Koukoulas and G. A. Blackburn, Introducing New Indices for Accuracy Evaluation of Classified Images Representing Semi-Natural Woodland Environments., *Photogramm Eng Remote Sensing*, vol. 67, pp. 499–510, 2001.
- [80] F. Canters, Evaluating the Uncertainty of Area Estimates Derived from Fuuy Land-Cover Classification.
- [81] R. G. Congalton and K. Green, Assessing the Accuracy of Remotely Sensed Data. CRC Press, 2019. <https://doi.org/10.1201/9780429052729>.
- [82] S. Jalayer, A. Sharifi, D. Abbasi-Moghadam, A. Tariq, and S. Qin, Modeling and Predicting Land Use Land Cover Spatiotemporal Changes: A Case Study in Chalus Watershed, Iran, *IEEE J Sel Top Appl Earth Obs Remote Sens*, vol. 15, pp. 5496–5513, 2022, <https://doi.org/10.1109/JSTARS.2022.3189528>.
- [83] J. Wright, T. M. Lillesand, and R. W. Kiefer, Remote Sensing and Image Interpretation, *Geogr J*, vol. 146, no. 3, p. 448, 1980, <https://doi.org/10.2307/634969>.
- [84] A. SINGH, Review Article Digital change detection techniques using remotely-sensed data, *Int J Remote Sens*, vol. 10, no. 6, pp. 989–1003, 1989, <https://doi.org/10.1080/01431168908903939>.
- [85] K. M. Brown, Per-pixel uncertainty in change detection using airborne remote sensing, Doctoral Thesis, University of Southampton, Southampton, 2005.
- [86] I. Vorovencii, Long-term land cover changes assessment in the Jiului Valley mining basin in Romania, *Front Environ Sci*, vol. 12, 2024, <https://doi.org/10.3389/fenvs.2024.1320009>.
- [87] A. A. Omeer, R. R. Deshmukh, R. S. Gupta, and J. N. Kayte, Land Use and Cover Mapping Using SVM and MLC Classifiers: A Case Study of Aurangabad City, Maharashtra, India, pp. 482–492, 2019. [https://doi.org/10.1007/978-981-13-9187-3\\_43](https://doi.org/10.1007/978-981-13-9187-3_43).
- [88] I. Vorovencii, Comparing the Performance of Different Classification Algorithms for Mapping and Assessing Land Cover Changes in Areas with Surface Mining and Complex Landscape Using Landsat Imagery, 2023. <https://doi.org/10.20944/preprints202305.1345.v1>.
- [89] B. R. Deilmai, B. Bin Ahmad, and H. Zabihi, Comparison of two Classification methods (MLC and SVM) to extract land use and land cover in Johor Malaysia, *IOP Conf Ser Earth Environ Sci*, vol. 20, p. 012052, 2014, <https://doi.org/10.1088/1755-1315/20/1/012052>.

